

## Research highlights

Cite this: *Lab Chip*, 2013, 13, 3989

Received 15th August 2013,

Accepted 15th August 2013

DOI: 10.1039/c3lc90091f

www.rsc.org/loc

Arghya Paul,<sup>abc</sup> Vincent Pisano,<sup>ab</sup> Alessandro Polini,<sup>ab</sup> Mehmet R. Dokmeci<sup>ab</sup>  
and Ali Khademhosseini<sup>\*abcd</sup>

## Fabrication of nanofibres using bioinspired microfluidic spinning

The fabrication of micro- and nanoscale fibres have garnered a lot of attention within the biomedical engineering community due to their diverse applications in the field of tissue engineering and regenerative medicine.<sup>1</sup> With their unique nanotopography and biomimetic architecture, fibres present a platform akin to the native extracellular matrix (ECM) environment and allow better control of the cellular behavior (such as attachment, proliferation and differentiation). In recent years, several methods have been introduced to produce different types of biocompatible fibres in a continuous manner. These approaches include electrospinning and microfluidic spinning, which generate fibres with a homogeneous chemical composition. However, these technologies are not easily adaptable to generate highly ordered and stable fibres with variable dimensions. To develop an ECM-mimicking scaffold, it is important to have a technology that can fabricate fibres with controlled structural features in a continuous manner.<sup>2</sup>

Inspired by the spinning mechanism of a silkworm, Lee and colleagues<sup>3</sup> have recently developed a strategy to generate fibres with tunable morphological and biofunctional properties. To demonstrate their approach, Chae *et al.*<sup>3</sup> used a non-toxic polysaccharide, alginate, as the model polymer. The schematic illustrations in Fig. 1a and b demonstrate the spinning duct of a silkworm where the fibroin protein is first produced at the posterior division, then gradually transferred to the middle division where the fibroin solution is concentrated to form micelle-like globular aggregates. These aggregates become oriented and stretched due to the physical shearing effects in the narrow duct. Finally, crystallization

induces silk fibre formation from the globular protein structures due to the combined effect of shear stress and dehydration of the aqueous phase in the anterior portion of the spinning duct.

Mimicking the natural fibre spinning procedure of the silkworm, a fibre spinning microfluidic device was devised

## (a) Spinning Duct of Silkworm

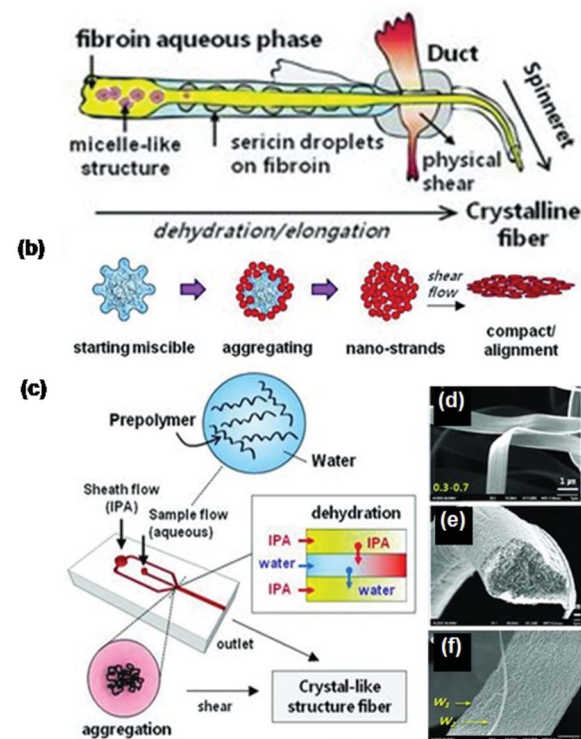


**Fig. 1** (a) Schematic illustration of a silkworm's spinning duct. (b) Basic mechanism of dehydration process of aqueous ionic polymer to form aggregates, eventually leading to nanostrands and highly ordered crystalline fibre formation due to shear stress. (c) The microfluidic system, mimicking the silkworm's spinning duct, consisting of two inlet channels and one outlet channel, with a core aqueous alginate and an outer IPA sheath flow. Scanning electron microscope images of nanofibres with different dimensions and morphologies (d, e, and f). Figure adapted and reprinted with permission from Chae *et al.*<sup>3</sup>

<sup>a</sup>Center for Biomedical Engineering, Department of Medicine, Brigham and Women's Hospital, Harvard Medical School, Cambridge, Massachusetts 02139, USA.

E-mail: alik@rics.bwh.harvard.edu

<sup>b</sup>Harvard-MIT Division of Health Sciences and Technology, Massachusetts Institute of Technology, Cambridge, Massachusetts 02139, USA

<sup>c</sup>Wyss Institute for Biologically Inspired Engineering, Harvard University, Boston, Massachusetts 02115, USA

<sup>d</sup>World Premier International – Advanced Institute for Materials Research (WPI-AIMR), Tohoku University, Sendai 980-8577, Japan

## Highlight

that consisted of two inlet and one outlet channels (Fig. 1c). The main microchannel had an initial width of 100  $\mu\text{m}$  which tapered to an intersection point with a 30  $\mu\text{m}$  width. Aqueous alginate prepolymer solution was used as the core fluid stream surrounding the flow to initiate the spinning process and water-miscible isopropyl alcohol (IPA) solvent was used as the sheath fluid at the junction. IPA has low polarity and can induce aggregate formation of ionic polymers, such as alginate, due to the dipole–dipole attractions at the dehydrating interface between the aqueous alginate core and the outer IPA sheath fluid.

Thus, as the dehydration by the IPA flow gradually progressed towards the core alginate flow, the alginate polymer chains aggregated towards the outlet, similar to the micelle-like fibroin globular aggregate formation at the anterior end of the silkworm's spinning duct. The shear force on the aggregates inside the microchannel helped to form densely packed and aligned nanostrands, eventually leading to the generation of highly ordered, mechanically strong alginate fibres with varying dimensions. By adjusting the flow rate of IPA and alginate in the microchannels, highly compact fibres with different geometries such as cylindrical, semi-cylindrical, seaweed-like and ultrathin structures were obtained. Additionally, the study demonstrated the generation of fibres with different dimensions through a single misaligned microchannel using the principle of Kelvin–Helmholtz instabilities which occur as a function of interfacial tension between the miscible fluids with different densities and velocities. Moreover, by varying the flow rates in the misaligned microchannel, multiple fibres with diverse morphologies were obtained.

These alginate nanofibres can be particularly useful to fabricate scaffolds which possess biomechanical functionality and strength to deliver sustainable micro-strains to cells and tissues.<sup>4</sup> Moreover, the free carboxylic acids on the alginate polymer backbone can be chemically modified with functional peptide molecules to promote cell–alginate interactions.

## Magnetically controlled rare cell isolation and release

The isolation of rare cells from blood has numerous biomedical applications. For instance, cell sorting can be used to isolate circulating tumor cells, detect viruses and diagnose prenatal disorders.<sup>5</sup> Typical cell sorting techniques, such as flow cytometry and immobilizing binding agents on microfluidic device surfaces, have their respective drawbacks of being inefficient or lacking cell release mechanisms.<sup>6</sup> Recently, Zhao and colleagues have developed a simple microfluidic device that uses magnetic nanoparticles (MNPs) for the capture and release of rare circulating cells.<sup>7</sup>

In their recent paper, Yu *et al.*<sup>7</sup> demonstrated an efficient capture and release strategy using magnetic fields. First, they fabricated nickel micropillar columns inside a microfluidic channel (Fig. 2). To create the MNPs,  $\text{Fe}_3\text{O}_4$  nanoparticles were

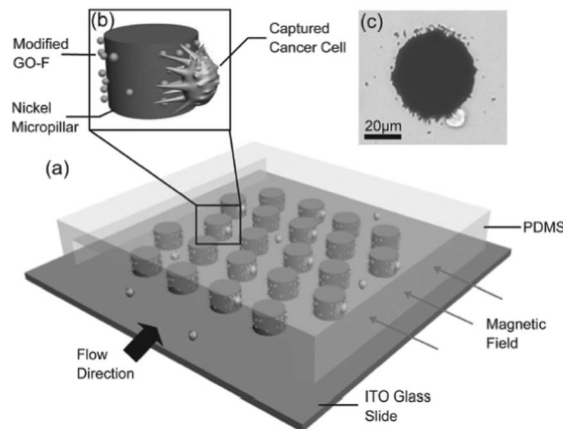


**Fig. 2** (a) Diagram of the microfluidic device decorated with nickel micropillars during cancer cell assay. (b) Schematic of a cancer cell binding to magnetic nanoparticles on a micropillar. (c) Image of a cancer cell binding to a micropillar during an actual experiment. Figure adapted and reprinted with permission from Yu *et al.*<sup>7</sup>

embedded in graphene oxide (GO) sheets by solution mixing. GO was chosen for its high stability and biocompatibility. Carboxyl groups on the  $\text{GO-Fe}_3\text{O}_4$  sheets were activated and conjugated with streptavidin, a molecule with high affinity to biotin. In this state the  $\text{GO-Fe}_3\text{O}_4$  sheets were primed for functionalization with biotinylated antibodies specific to the cells under investigation. Two permanent magnets were placed on either side of the microchannel generating a magnetic field perpendicular to the flow. Magnetic flux density was calculated to be largest near the top and the bottom of the pillars parallel to the magnetic field and was confirmed by running fluorescent MNPs through the device. The fluorescent MNPs were trapped at the upper and lower regions around each micropillar parallel to the magnetic field. Turning off the magnetic field was able to release the MNPs from their trapped sites.

To test their device, the authors designed an experiment to determine the device's capture efficiency of rare cells suspended in a medium. HCT116 colorectal cancer cells were chosen because they overexpress an antigen called epithelial cell adhesion molecule (EpcAM).  $\text{GO-Fe}_3\text{O}_4$  MNPs ( $\text{GO-F}$ ) sheets conjugated with streptavidin were incubated with biotinylated anti-EpcAM so that the cells in transit expressing EpcAM were attracted to the MNPs *via* cell affinity. The anti-EpcAM-MNPs were suspended in a PBS solution, injected into the device and the magnetic field was applied. The HCT116 cells were next suspended in a culture medium, injected into the device and the captured cells were inspected by a microscope. To release the captured cells, the magnetic field was turned off and the device was washed with PBS. The microfluidic device exhibited a capture rate  $>70\%$  for the HCT116 cells in the medium. The device's capture rate was enhanced by the clever design of the interaction between the cells and the micropillars *via* the use of high density  $\text{GO-Fe}_3\text{O}_4$  binding sites.

The efficiency of the device was based on three key factors: pillar diameter, pillar height and flow rate. The optimal pillar diameter was experimentally determined to be 50  $\mu\text{m}$ . Micropillar heights were controlled simply by adjusting the electroplating times. Capture efficiencies rose with increasing micropillar heights of up to 10  $\mu\text{m}$  and then reached a saturation point. Yu *et al.*<sup>7</sup> surmised that this observation was due to both the average diameter of the cancer cells being 8–10  $\mu\text{m}$  and the cancer cells precipitating to the bottom of microchannel. Since the cancer cells were about the same height as the micropillars and the MNPs were distributed to the top and bottom of the micropillars, the cancer cells were able to bind to the MNPs on both the top and the bottom maximizing capture efficiency. A flow rate of 50  $\mu\text{L h}^{-1}$  or below was found to be optimal as the cells precipitated to the bottom of the channel at this flow rate. Capture efficiency was significantly decreased at flow rates above 100  $\mu\text{L h}^{-1}$  due to the reduced interactions between the cells and the micropillars.

A unique aspect of this device is the ease in releasing the captured cells. By removing the permanent magnets and washing the sample with PBS, the MNP-cancer cells were readily released from the micropillars. About 93% of the captured cells were released while some cells remained trapped by the residual magnetic flux density in the nickel micropillars. The released cells had a high viability of about 78% as confirmed by the fluorescein diacetate and propidium iodide staining (a probe that measures enzyme activity and cell viability). Additionally, even with the MNPs still attached to the cells, the analysis of the cellular DNA and RNA content can still proceed. This reusable device offers an affordable and advantageous alternative to traditional cell sorting and will inspire new applications in diagnostics, therapeutics and biotechnology.

## Modular microfluidic systems using PDMS control valves

Microfluidic systems enable the manipulation of fluids generally in a highly accurate way in very small volumes, often at the nanoliter scale. The application of microfluidic technologies for high-throughput studies as well as the development of new analytical devices have led to the design and fabrication of sophisticated systems.<sup>8</sup> Proper control of fluid movements in these systems has required significant technological efforts.<sup>9</sup> For example, monolithic PDMS micro-mechanical valves, are popular and attractive due to their ease of fabrication, low cost and scalability. These valves have found applications in several fields, such as protein crystallography, genetic analysis, high-throughput screening, and chemical synthesis.<sup>9</sup> Recent technological advances have led to the development of microfluidic very large scale integration (mVLSI) with an astonishing number of integrated valves (thousands of valves per  $\text{cm}^2$ ).<sup>8</sup>

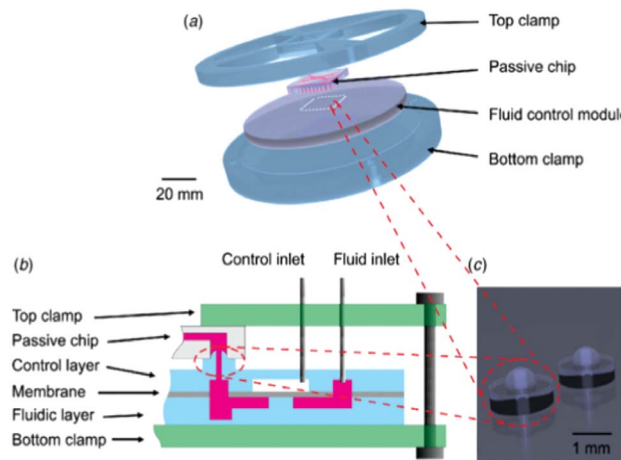


**Fig. 3** Schematic of the modular hybrid microfluidic system. (a) Expanded view showing the passive PMMA chip, the PDMS fluid control module and the clamps. (b) The cross-sectional view of the system. (c) Images of the modular hybrid microfluidic systems. Figure adapted and reprinted with permission from Skafte-Pedersen *et al.*<sup>10</sup>

On the other hand, modular systems represent an interesting alternative to the large scale integration approach. By fabricating and assembling modular elements, complex systems can be created without the need for redesigning and/or refabricating the entire microfluidic system (a crucial point during the prototyping phase). To create modular systems, an important challenge is the development of hybrid systems which allow reversible bonding between different devices with a standardized interconnection scheme. Recently, Skafte-Pedersen *et al.*<sup>10</sup> reported a modular hybrid system with a universal soft lithography-based fluidic control module interfaced to an external hard polymeric chip. This system consisted of different modular elements (Fig. 3): i) a three-layer PDMS-based fluidic control module fabricated by soft lithography and controlled pneumatically; ii) a hard passive PMMA chip, having a 2D chamber with  $4 \times 8$  interconnections; iii) a polycarbonate clamping system as the mechanical support to the chip-to-control module interconnection, that assures very small variations in the flow rate with no leaks. The system is completed by integrating O-rings, enabling the control of module-hard chip fluidic interconnections and allowing the reversible sealing of the elements. The platform offers a robust flow control in two dimensions using external PDMS valves in a fully passive microfluidic PMMA chip, as demonstrated with complex on-chip fluid patterns through the 2D chamber. Interestingly, the authors showed that the assembly of several elements does not affect the performance in terms of flow stability as the O-ring-based interconnection scheme provided robust sealing of the overall platform.

Though currently simpler than the high density microscale integrated systems present in the literature (lower valve density in comparison to monolithic systems), this approach presents an interesting modular concept and an interconnection scheme and can be the starting point for the generation of

more complex microfluidic devices. Moreover, a variety of different applications can potentially be envisioned for these systems, thanks to their flexibility in terms of materials, integratable elements and configurations.

## References

- 1 S. Prakash, A. Khan and A. Paul, *Expert Opin. Biol. Ther.*, 2010, **10**, 1649–1661.
- 2 E. Kang, G. S. Jeong, Y. Y. Choi, K. H. Lee, A. Khademhosseini and S. H. Lee, *Nat. Mater.*, 2011, **10**, 877–883.
- 3 S. K. Chae, E. Kang, A. Khademhosseini and S. H. Lee, *Adv. Mater.*, 2013, **25**, 3071–3078.
- 4 J. M. Coburn, M. Gibson, S. Monagle, Z. Patterson and J. H. Elisseeff, *Proc. Natl. Acad. Sci. U. S. A.*, 2012, **109**, 10012–10017.
- 5 P. Wulfing, J. Borchard, H. Buerger, S. Heidl, K. S. Zanker, L. Kiesel and B. Brandt, *Clin. Cancer Res.*, 2006, **12**, 1715–1720.
- 6 J. Chen, J. Li and Y. Sun, *Lab Chip*, 2012, **12**, 1753–1767.
- 7 X. Yu, R. He, S. Li, B. Cai, L. Zhao, L. Liao, W. Liu, Q. Zeng, H. Wang, S. S. Guo and X. Z. Zhao, *Small*, 2013, DOI: 10.1002/smll.201300169.
- 8 I. E. Araci and S. R. Quake, *Lab Chip*, 2012, **12**, 2803–2806.
- 9 J. Melin and S. R. Quake, *Annu. Rev. Biophys. Biomol. Struct.*, 2007, **36**, 213–231.
- 10 P. Skafte-Pedersen, C. G. Sip, A. Folch and M. Dufva, *J. Micromech. Microeng.*, 2013, **23**, 055011.